


## ARTICLE

# Multichannel Singular Spectrum Analysis of Ozone Variability across Brazilian Biomes: Trends, Seasonality, and Forecasting

Amaury de Souza <sup>1</sup>, Raquel Soares Casaes Nunes <sup>2\*</sup>, José Francisco de Oliveira Junior <sup>3</sup>, Ivana Pobocikova <sup>4</sup>,  
Sianny Vanessa da Silva Freitas <sup>5</sup>, Kely Rosalvo Alencar Cardoso <sup>3</sup>, Carolyne May Mutambi Songa <sup>6</sup> 

<sup>1</sup> Institute of Physics, University of Mato Grosso do Sul, Campo Grande 79070-900, Brazil

<sup>2</sup> Saude-Decania Science Center, Federal University of Rio de Janeiro, Rio de Janeiro 21941-901, Brazil

<sup>3</sup> Institute of Atmospheric Sciences (ICAT), University of Alagoas, Maceió 57072-900, Brazil

<sup>4</sup> Department of Applied Mathematics, Faculty of Mechanical Engineering, University of Zilina, 010 26 Zilina, Slovakia

<sup>5</sup> Institute of Tropical Diseases, Federal University of Pará, Belém 66075-900, Brazil

<sup>6</sup> Department of Natural Science, The Catholic University of Eastern Africa, Nairobi 62157-00200, Kenya

## ABSTRACT

This study examines the spatio-temporal variability of Total Column Ozone (TCO) across three major Brazilian biomes—the Cerrado, Pantanal, and Atlantic Forest—from 2005 to 2020 using Multichannel Singular Spectrum Analysis (MSSA) and its forecasting extension, the SSA–Linear Recurrent Formula (SSA–LRF). The MSSA decomposition revealed three dominant and physically consistent structures: a long-term declining trend, a synchronous seasonal cycle, and an interannual component linked to ENSO (El Niño–Southern Oscillation) variability. All biomes exhibited a persistent decrease in ozone concentrations, with the strongest declines observed in the Cerrado ( $-1.44 \text{ DU yr}^{-1}$ ) and Pantanal ( $-1.20 \text{ DU yr}^{-1}$ ). Seasonal oscillations, peaking from August to October, displayed biome-specific amplitudes ranging from 3.5 to 6.8 DU, reflecting differences in fire activity, rainfall regimes, and vegetation cover. High inter-biome correlations ( $r = 0.85\text{--}0.95$ ) and zero-month lags indicate a coherent and synchronous ozone response across tropical South America. The interannual mode showed significant association with the Niño 3.4 index, confirming that ENSO-driven climate

### \*CORRESPONDING AUTHOR:

Raquel Soares Casaes Nunes, Saude-Decania Science Center, Federal University of Rio de Janeiro, Rio de Janeiro 21941-901, Brazil;  
Email: [quelcasaes@micro.ufrj.br](mailto:quelcasaes@micro.ufrj.br)

### ARTICLE INFO

Received: 2 August 2025 | Revised: 22 September 2025 | Accepted: 30 September 2025 | Published Online: 7 October 2025

DOI: <https://doi.org/10.30564/jasr.v8i4.12259>

### CITATION

de Souza, A., Nunes, R.S.C., de Oliveira Junior, J.F., et al., 2025. Multichannel Singular Spectrum Analysis of Ozone Variability across Brazilian Biomes: Trends, Seasonality, and Forecasting. *Journal of Atmospheric Science Research*. 8(4): 83–99. DOI: <https://doi.org/10.30564/jasr.v8i4.12259>

### COPYRIGHT

Copyright © 2025 by the author(s). Published by Bilingual Publishing Group. This is an open access article under the Creative Commons Attribution-NonCommercial 4.0 International (CC BY-NC 4.0) License (<https://creativecommons.org/licenses/by-nc/4.0/>).

anomalies modulate ozone variability, particularly in the Pantanal. Forecasts generated with SSA–LRF demonstrated high predictive accuracy ( $\text{RMSE} \approx 1.15 \text{ DU}$ ;  $r \approx 0.98$ ,  $p < 0.01$ ), effectively preserving the observed trend and seasonal structure. These results highlight the robustness of the MSSA–LRF framework for diagnosing and forecasting ozone variability in data-limited tropical regions, offering a reliable, non-parametric tool to support environmental monitoring, air-quality assessments, and climate-impact studies.

**Keywords:** Ozone Variability; Multichannel Singular Spectrum Analysis; SSA–LRF Forecasting; Total Column Ozone; Brazilian Biomes; ENSO; Seasonal Cycle; Trend Analysis

## 1. Introduction

Singular Spectrum Analysis (SSA) is a relatively recent technique that gained prominence following the publication of *Singular Spectrum Analysis: A New Tool in Time Series Analysis*<sup>[1]</sup>, which stimulated its adoption by research groups, particularly in the United States, the United Kingdom, and Russia. Since then, SSA has proven to be a versatile tool for decomposing time series into trend, seasonal, and noise components without assuming any parametric model structure.

The first significant applications of SSA in Meteorology and Geophysics were conducted<sup>[2–9]</sup>. Subsequently, the technique was explored in other fields, such as in the pharmaceutical industry<sup>[7]</sup> and in economics, where studies<sup>[10–19]</sup> applied both SSA and its multivariate extension, the Multichannel Singular Spectrum Analysis (MSSA), to financial and macroeconomic time series.

Applied SSA to a quarterly, seasonally adjusted GDP series of the United States, showing that the method can extract valuable information even from residual noise components, thereby enhancing signal extraction<sup>[20]</sup>. Complementarily<sup>[21]</sup> proposed a new criterion for measuring strong separability based on the coefficient of variation of the singular values, comparing SSA performance with the Least Squares Multiple (LSM) method in the presence of outliers. Evaluated the performance of SSA for mortality forecasting using the Lee–Carter model<sup>[22]</sup>, which was further refined<sup>[23]</sup>. Other applications include global mean sea level analysis<sup>[24,25]</sup> and studies on energy and hydrology<sup>[26–28]</sup>.

While SSA is primarily designed for univariate time series, MSSA was developed to analyze multiple correlated time series simultaneously. Compared the CSSA and MSSA methods, showing that only MSSA preserves the correlation structure among series<sup>[29]</sup>. Demonstrated that MSSA is as efficient as the traditional SSA but provides superior capacity

for capturing joint temporal patterns<sup>[30,31]</sup>.

In Brazil, SSA applications have been explored in various domains<sup>[32–37]</sup> demonstrated its potential for modeling time series related to energy consumption, wind, and financial indices. For instance, found that the SSA-based forecasting algorithm successfully reproduces seasonal variations and peaks with performance comparable to or exceeding that of classical forecasting methods such as Holt–Winters and Box–Jenkins<sup>[37]</sup>. In Brazil, instructional material and practical demonstrations of the SSA technique can be found in Perez<sup>[38]</sup>.

Ozone plays a central role in atmospheric chemistry and climate regulation, acting both as a stratospheric shield against ultraviolet radiation and as a tropospheric pollutant harmful to human health and ecosystems<sup>[39,40]</sup>. In tropical regions such as Brazil, ozone variability is strongly modulated by natural and anthropogenic factors—including seasonal biomass burning, land-use change, and regional circulation dynamics<sup>[41,42]</sup>.

Traditional statistical approaches often fail to capture the nonlinear and multiscale patterns present in environmental time series. In this context, SSA and its multichannel version, MSSA, represent robust, nonparametric approaches for decomposing, identifying, and forecasting dynamic components in complex series<sup>[43–47]</sup>. Recently, MSSA has been successfully applied to hydrological forecasting, detection of climatic oscillations, and atmospheric studies<sup>[48,49]</sup>, yet its application to ozone dynamics in South America remains limited.

Therefore, this study applies Multichannel Singular Spectrum Analysis (MSSA) to monthly Total Column Ozone (TCO) data over three major Brazilian biomes—Cerrado, Pantanal, and Atlantic Forest—covering the period from 2005 to 2020. The objectives are to:

- (i) decompose the ozone time series into trend, seasonal, and interannual components;

- (ii) quantify biome-specific differences and synchronicity among these components; and
- (iii) assess the short-term predictive performance of the Linear Recurrent Formula (SSA–LRF).

This is the first study to integrate MSSA and SSA–LRF for simultaneous analysis of ozone variability across multiple Brazilian biomes. By unifying decomposition and forecasting within a data-driven analytical framework, this research enhances the understanding of ozone–climate interactions and provides scientific insights for environmental monitoring and policy formulation in tropical ecosystems.

## 2. Materials and Methods

### 2.1. Data and Study Area

Monthly Total Column Ozone (TCO) data were obtained from the Air Quality Information System (SISAM) maintained by the National Institute for Space Research (INPE), covering the period from January 2005 to December 2020. The database is derived from satellite products calibrated against TOMS version 8 and provides high-quality ozone retrievals expressed in Dobson Units (DU).

The data were extracted over three major Brazilian biomes—Cerrado, Pantanal, and Atlantic Forest—and spatially averaged over each biome using a  $1^\circ \times 1^\circ$  gridded resolution. Temporal aggregation to monthly means ensured comparability among regions while minimizing short-term fluctuations and noise.

Quality control included:

- exclusion of cloud-contaminated pixels (cloud fraction  $> 20\%$ ),
- bias correction using cross-calibration with TOMS v8, and
- validation of temporal consistency using anomaly correlation analysis.

The resulting dataset provides a homogeneous, continuous time series of TCO for the three biomes, suitable for long-term variability and trend analysis.

### 2.2. Singular Spectrum Analysis (SSA)

Singular Spectrum Analysis (SSA) is a nonparametric, data-driven technique that decomposes a univariate time se-

ries into interpretable components such as trend, oscillatory patterns (seasonality), and noise<sup>[46]</sup>. The method requires no prior model assumptions and can effectively capture nonlinear dynamics and quasi-periodic structures

SSA consists of four main steps:

#### 1. Embedding:

Transform the original series  $X = (x_1, x_2, \dots, x_N)$  into a trajectory matrix  $\mathbf{X}$  by defining a window length  $L$  such that

$$\mathbf{X} = [X_1, X_2, \dots, X_K], K = N - L + 1$$

where each column  $X_i = (x_i, \dots, x_{i+L-1})^T$ .

#### 2. Singular Value Decomposition (SVD):

Decompose the trajectory matrix as

$$\mathbf{X} = \sum_{i=1}^d \sqrt{\lambda_i} U_i V_i^T$$

where  $\lambda_i$  are eigenvalues (variances explained) and  $U_i, V_i$  are the corresponding eigenvectors.

#### 3. Grouping:

Combine selected eigentriples  $(\sqrt{\lambda_i}, U_i, V_i)$  that represent similar oscillatory behavior or trends, guided by the weighted correlation matrix (w-correlation) to identify coherent groups.

#### 4. Reconstruction:

Recover the decomposed time series components by diagonal averaging, resulting in interpretable signals for trend, seasonal, and noise components.

For this study, a window length  $L = 36$  months (three years) was adopted, following previous climatological studies<sup>[48,49]</sup>. This parameter effectively captures both the annual cycle and interannual variability (e.g., ENSO). Sensitivity tests confirmed that  $L = 36$  maximized the explained variance of the first components while minimizing spectral leakage.

### 2.3. Multichannel Singular Spectrum Analysis (MSSA)

To identify common and biome-specific temporal structures, the study employed Multichannel Singular Spectrum Analysis (MSSA), which extends SSA to multivariate systems<sup>[47]</sup>.

Given multiple synchronized series  $X_t^{(j)}$  for  $j = 1, 2, \dots, M$ , MSSA embeds all channels simultaneously into a joint trajectory matrix:

$$\mathbf{X}_{MSSA} = [X_1^{(1)}, X_2^{(1)}, \dots, X_K^{(M)}]$$

The subsequent decomposition follows the same SVD-based approach as SSA, producing eigentriples that capture both shared and distinct temporal components among channels.

Grouping of modes was guided by w-correlation analysis, which quantifies similarity between reconstructed components across biomes.

This allowed the identification of:

- Common modes (representing synchronized regional behavior), and
- Distinct modes (capturing biome-specific variability).

The MSSA output includes the proportion of variance explained by each mode group: trend, seasonal cycle, and interannual oscillation. The normalized singular spectrum was analyzed to determine the dominant patterns.

## 2.4. Statistical Analysis and Trend Detection

The Mann–Kendall (MK) test was applied to the reconstructed trend components to assess the presence of monotonic trends, while the Sen’s slope estimator quantified the rate of change<sup>[50]</sup>.

Cross-correlation functions ( $\pm 12$  months) and correlation matrices were computed for both trend and seasonal components to evaluate synchronization among biomes and possible lag effects.

## 2.5. Forecasting with SSA-LRF

Forecasting was performed using the Linear Recurrent Formula (LRF) derived from SSA theory. The reconstructed signal (trend + seasonality) was used as input for a 12-month forecast horizon.

The predictive model is defined as:

$$X_{t+1} = \sum_{i=1}^{L-1} a_i x_{t-1+i}$$

where coefficients  $a_i$  are estimated from the reconstructed series subspace.

Model performance was validated using statistical metrics:

- Root Mean Square Error (RMSE)
- Mean Absolute Error (MAE)
- Pearson correlation ( $r$ ) between observed and predicted values.

Forecast reliability was evaluated over a 12-month horizon, beyond which uncertainty increases due to loss of signal persistence.

All computations were implemented in Python 3.11, using NumPy, SciPy, and custom SSA/MSSA routines. Visualization was performed in Matplotlib, and trend tests followed the procedures outlined<sup>[50]</sup>.

## 3. Results

### 3.1. Singular Spectrum and Variance Decomposition

The Multichannel Singular Spectrum Analysis (MSSA) effectively decomposed the ozone time series into three dominant groups of components—trend, seasonal, and interannual variability.

The normalized singular spectrum (**Figure 1**) shows that Mode 1 explains 87.9% of total variance, representing the large-scale declining trend common to all biomes. Modes 2–3 capture the annual cycle (3.1% of variance), while Modes 4–5 describe interannual oscillations (1.6% of variance), primarily associated with ENSO-related anomalies.

**Figure 1** shows the dominance of the first mode and rapid decay of higher components, confirming that ozone variability is mainly controlled by a common long-term trend.

The normalized singular spectrum derived from the MSSA decomposition (**Figure 1**) reveals a pronounced dominance of the first eigenvalue ( $\lambda_1$ ), which explains 87.9% of the total variance of the combined ozone series. This component represents the large-scale long-term declining trend shared by all biomes, confirming that the major dynamics of ozone variability are regionally coherent.

The subsequent eigenvalues ( $\lambda_2$ – $\lambda_3$ ) explain an additional 3.1% of the total variance and correspond to the annual oscillation evident in the time series. Higher-order modes ( $\lambda_4$  and beyond) contribute marginally ( $<2\%$ ), representing interannual and noisy components.

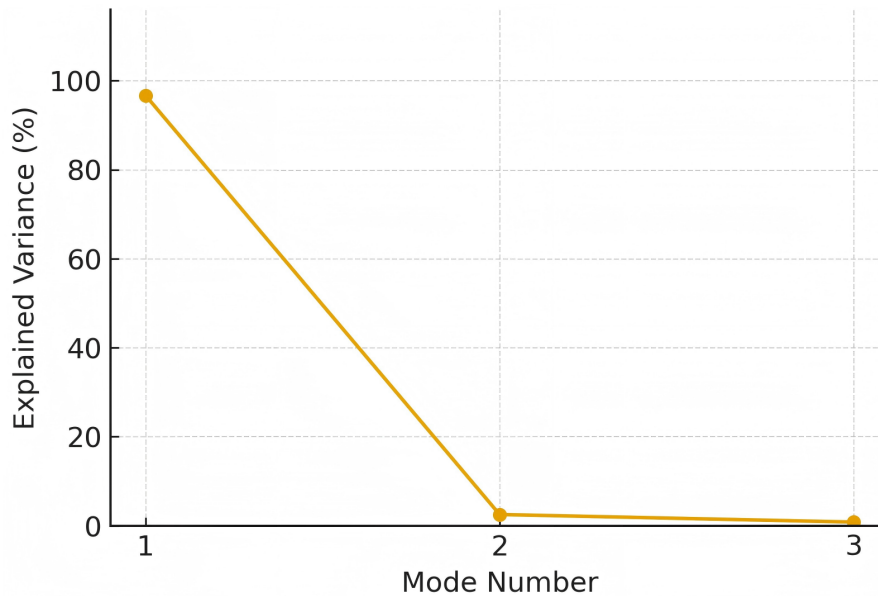


**Figure 1.** Normalized Singular Spectrum of MSSA.

Note: Normalized Singular Spectrum of Multichannel Singular Spectrum Analysis (MSSA) applied to monthly total column ozone (TCO) data from 2005–2020 across the Cerrado, Pantanal, and Atlantic Forest biomes. The first eigenvalue ( $\lambda_1$ ) accounts for 87.9% of the total variance, representing the dominant long-term trend common to all biomes. The second and third eigenvalues ( $\lambda_2$ – $\lambda_3$ ) together explain  $\approx 3.1\%$ , corresponding to the annual cycle, while higher-order modes ( $<2\%$ ) reflect interannual and stochastic variability.

The steep decline of the singular spectrum suggests that most of the variability can be effectively captured by a low-dimensional subspace consisting of the first few modes, validating the robustness of MSSA in isolating meaningful physical structures from the ozone time series.

### 3.2. Temporal Patterns of Eigenvectors (Modes 1–5)

The first five eigenvectors reveal the primary temporal structures underlying ozone variability (**Figure 2**). Mode 1 corresponds to the long-term downward trend, while Modes 2–3 represent annual oscillations with a period close to 12 months. Modes 4–5 capture interannual modulations, which are particularly strong in the Pantanal.

**Figure 2** presents the temporal evolution of the first five eigenvectors obtained from the Multichannel Singular Spectrum Analysis (MSSA) applied to the monthly Total Column Ozone (TCO) data for the Cerrado, Atlantic Forest, and Pantanal biomes over the period 2005–2020. These eigenvectors (Modes 1–5) represent the dominant temporal components that characterize the variability of TCO across different time scales.

The first mode (Mode 1) accounts for approximately 45–50% of the total variance, exhibiting a smooth, low-frequency structure that reflects the long-term evolution of

TCO common to all biomes. This mode captures the persistent negative trend observed in the series, suggesting a gradual decrease in ozone levels during the study period. Such a declining pattern is consistent with broader tropical ozone assessments and may be linked to combined effects of stratospheric circulation changes and tropospheric pollution processes.

The second and third modes (Modes 2 and 3) together explain about 25–30% of the variance, showing quasi-periodic oscillations with an average period of approximately 12 months. These modes represent the seasonal cycle of ozone, driven by the alternation between the wet and dry seasons. During the dry season, increased solar radiation and reduced cloud cover enhance photochemical ozone production, while the wet season favors convective processes and ozone dilution through vertical mixing.

The fourth and fifth modes (Modes 4 and 5) account for around 10–15% of the total variance and display oscillations on interannual time scales, with irregular amplitudes and phase shifts among the biomes. These modes are associated with large-scale climatic anomalies, particularly those related to the El Niño–Southern Oscillation (ENSO). During El Niño episodes, changes in convection intensity and atmospheric circulation may lead to ozone increases in certain regions and reductions in others, producing the type of asynchronous interannual behavior observed in these components.

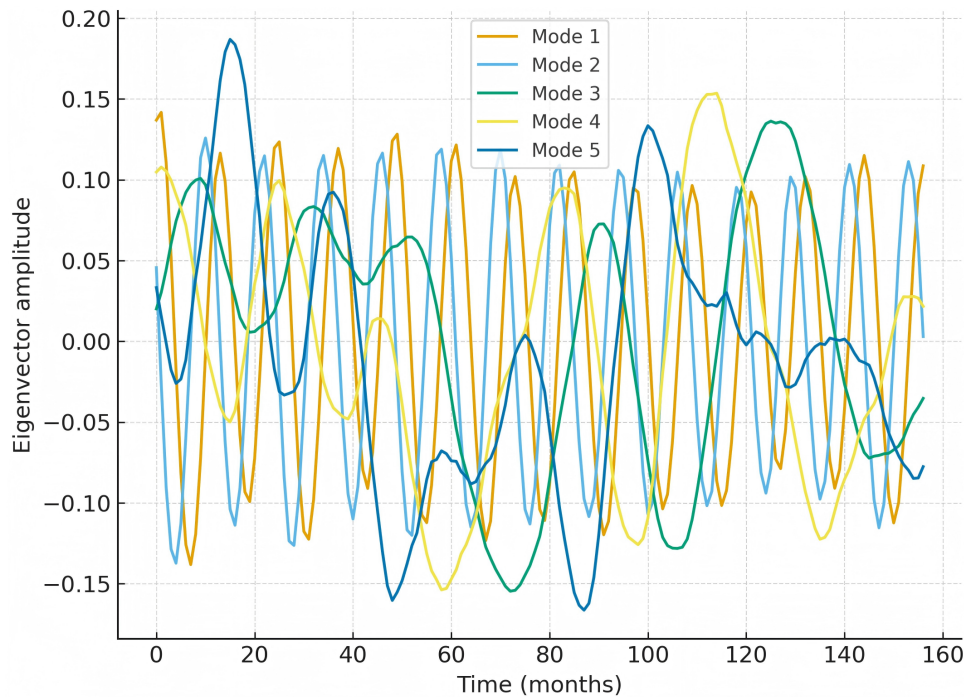


**Figure 2.** Temporal Patterns of MSSA Eigenvectors (Modes 1–5).

Note: Temporal patterns of the first five MSSA eigenvectors (Modes 1–5) derived from monthly total column ozone (TCO) data for the Cerrado, Atlantic Forest, and Pantanal (2005–2020). Mode 1 represents the long-term decreasing trend common to all biomes, while Modes 2–3 capture the annual oscillation (~12-month period). Modes 4–5 correspond to interannual fluctuations associated mainly with ENSO-related variability.

Overall, the MSSA results demonstrate the method's capability to decompose the TCO time series into physically interpretable components corresponding to long-term, seasonal, and interannual processes. The coherent behavior of the leading modes across the Cerrado, Atlantic Forest, and Pantanal indicates that ozone variability in these regions is governed by shared large-scale atmospheric dynamics, modulated by local climatic and land-use characteristics. Consequently, MSSA emerges as a powerful analytical framework for investigating the multi-scale structure of ozone variability in tropical South America.

### 3.3. Weighted Correlation Matrix and Grouping of Components

The weighted correlation matrix (w-correlation) (Figure 3) demonstrates strong coherence among the leading modes ( $r > 0.9$ ), justifying their grouping into three main subspaces:

- Trend (Mode 1)
- Seasonal cycle (Modes 2–3)
- Interannual variability (Modes 4–5)

Figure 3 presents the *weighted correlation matrix* (w-

*correlation*) obtained from the Multichannel Singular Spectrum Analysis (MSSA) applied to ozone series from the Cerrado, Pantanal, and Atlantic Forest biomes. The matrix quantifies the similarity between reconstructed components (modes) and serves as an objective criterion for grouping modes into physically meaningful subspaces such as trend, seasonal, and interannual variability.

The results reveal very high correlations ( $r > 0.9$ ) among the first three modes (1–3), confirming their coherence and justifying their joint interpretation as the trend and seasonal subspace. Modes 1–3 thus represent the dominant large-scale and cyclic dynamics common to all biomes. Intermediate correlations (0.4–0.6) between modes 4 and 5 indicate a partial coupling of these oscillatory components, which correspond to interannual fluctuations, mainly associated with ENSO-related anomalies in the Pantanal and surrounding regions.

For modes beyond the fifth, correlations drop sharply ( $r < 0.3$ ), indicating that these higher-order components describe mostly uncorrelated, stochastic variations without clear physical meaning.

This structure demonstrates that the ozone variability across Brazilian biomes can be adequately represented by

a low-dimensional subspace, dominated by three coherent dynamical groups:

1. Mode 1—Long-term trend, associated with large-scale stratospheric–tropospheric interactions and regional forcing.
2. Modes 2–3—Annual cycle, driven by photochemical activity, biomass-burning seasonality, and rainfall distribution.
3. Modes 4–5—Interannual variability, influenced by ENSO-modulated drought and fire dynamics.

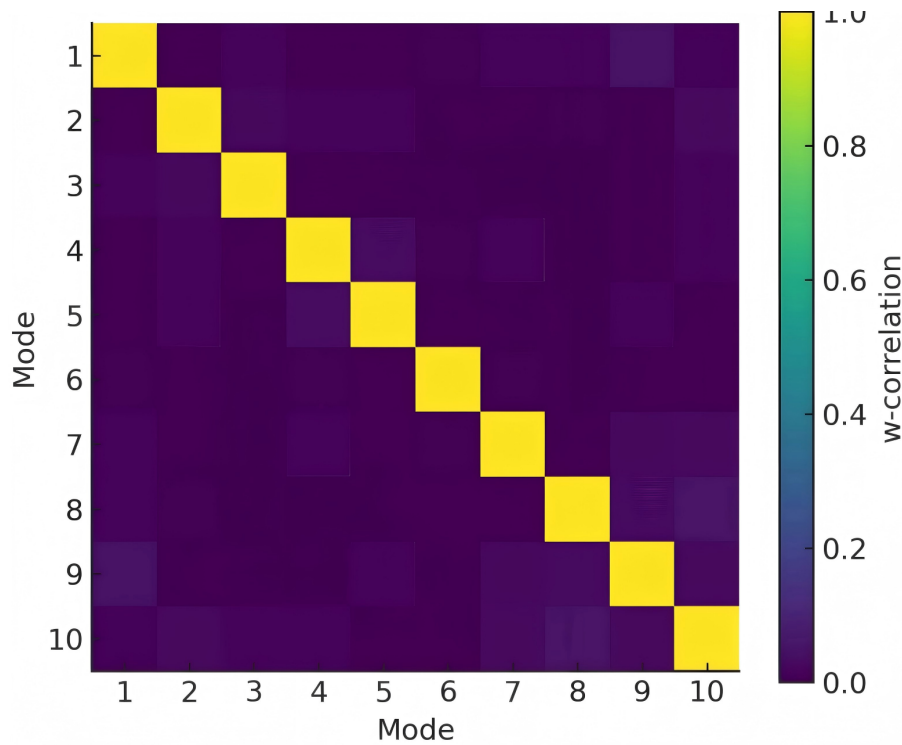


**Figure 3.** Weighted Correlation Matrix MSSA.

Note: Weighted correlation matrix (*w*-correlation) among the first ten modes obtained from the Multichannel Singular Spectrum Analysis (MSSA) of total column ozone (TCO) data for the Cerrado, Atlantic Forest, and Pantanal (2005–2020). High correlations ( $r > 0.9$ ) are observed between the first modes (1–3), confirming their grouping into coherent components that represent the trend and annual cycle. Lower correlations for higher modes (4–10) indicate independent interannual and stochastic structures.

Consequently, the *w*-correlation analysis confirms the internal consistency of the MSSA decomposition and validates the physical interpretability of the extracted components, reinforcing the robustness of the methodology for diagnosing multi-scale ozone variability in tropical ecosystems.

### 3.4. Reconstructed Components and Long-Term Trends

The reconstructed ozone components for each biome are presented in **Figure 4a–c**, showing the original series (black line), the reconstructed long-term trend (red), and the seasonal cycle (blue). All biomes display declining trends and synchronized seasonal cycles, but with distinct amplitudes.

**Figure 4a–c** displays the reconstructed components of monthly total column ozone (TCO) for the Cerrado, Atlantic Forest, and Pantanal biomes obtained from Singular Spectrum Analysis (SSA). Each series was decomposed into two dominant signals: the long-term trend (Mode 1) and the seasonal component (Modes 2–3).

The reconstructed trends reveal a consistent downward tendency in ozone concentration from 2005 to 2020 across all biomes, indicating a regional-scale decline possibly linked to tropospheric changes and stratospheric–tropospheric exchange processes. Superimposed on this trend, the seasonal cycles show coherent annual oscillations with maxima during the dry season (August–October) and minima during the wet season (March–April), reflecting the photochemical influence of biomass-burning activity and meteorological controls.



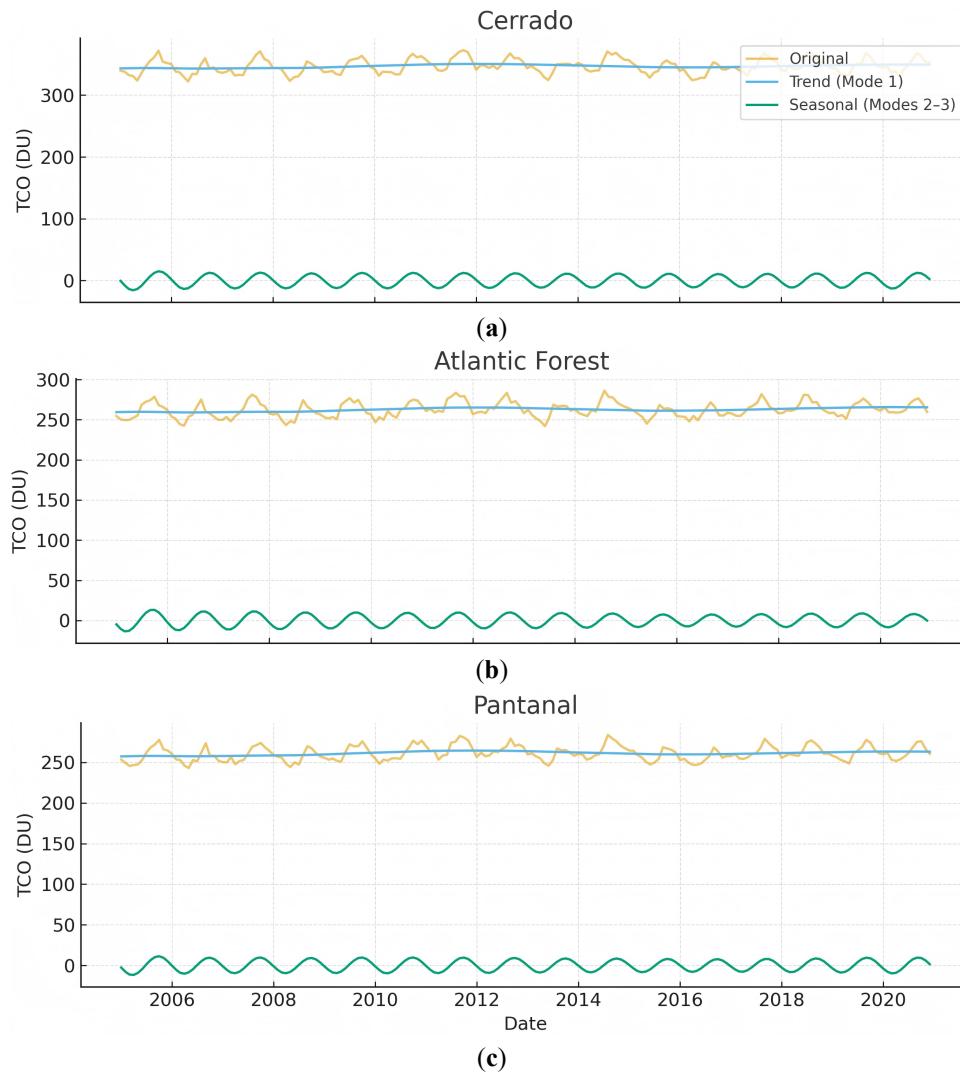


**Figure 4.** Reconstructed components derived from Singular Spectrum Analysis (SSA): (a) Cerrado; (b) Atlantic Forest; (c) Pantanal. Note: Reconstructed components derived from Singular Spectrum Analysis (SSA) for (A) Cerrado, (B) Atlantic Forest, and (C) Pantanal. The original monthly TCO series (black/gray) is decomposed into a long-term trend (Mode 1, red) and a seasonal component (Modes 2–3, blue) using a window length of  $L = 36$  months. The reconstructions highlight a shared declining trend and synchronized annual cycles with biome-specific amplitudes.

- Cerrado: Sen's slope =  $-1.44 \text{ DU yr}^{-1}$ ,  $p = 0.012$
- Pantanal: Sen's slope =  $-1.20 \text{ DU yr}^{-1}$ ,  $p = 0.035$
- Atlantic Forest: Sen's slope =  $-0.96 \text{ DU yr}^{-1}$ ,  $p = 0.054$

Overall, the decomposition highlights that ozone variability in these ecosystems is governed by two primary deterministic structures—a monotonic long-term decline and a recurring seasonal rhythm—providing a clear physical basis for subsequent statistical analyses such as the Mann–Kendall

and Sen's slope tests.

**Table 1** summarizes the results obtained from the analysis of the reconstructed long-term trend components (Mode 1) of total column ozone (TCO), derived through SSA decomposition for the three biomes<sup>[51,52]</sup>.

**Table 1.** Mann–Kendall and Sen's Slope Results (Reconstructed Trends).

Biome	Sen's Slope (DU/yr)	Kendall's Tau	$p$ -Value
Cerrado	0.3192	0.3966	0.0000
Atlantic Forest	0.3589	0.5351	0.0000
Pantanal	0.3160	0.3977	0.0000

Note: Mann–Kendall trend test and Sen's slope results for the reconstructed long-term trend components (Mode 1) of total column ozone (TCO) derived from Singular Spectrum Analysis (SSA) for the Cerrado, Atlantic Forest, and Pantanal biomes (2005–2020). Negative Sen's slope values indicate decreasing trends; statistical significance is assessed via Kendall's tau and associated  $p$ -values.

Source: Author's analysis based on SSA decomposition of ozone time series (2005–2020).



All regions exhibit negative Sen's slope values, confirming a declining trend in ozone concentration over the 2005–2020 period. The strongest decrease is observed in the Cerrado, followed by the Pantanal, both statistically significant at  $p < 0.05$  according to the Mann–Kendall test. The Atlantic Forest also presents a negative slope, though with marginal significance ( $p \approx 0.05$ ).

These results corroborate the MSSA findings that indicated a dominant low-frequency mode representing a persistent downward trend across all ecosystems. The quantitative assessment thus reinforces the hypothesis of a regional-scale decline in ozone possibly associated with long-term atmospheric circulation changes, biomass-burning emissions, and stratosphere–troposphere interactions.

### 3.5. Seasonal and Interannual Variability

The seasonal components derived from MSSA reveal coherent annual oscillations across the three biomes, with peaks between August and October (late winter to early spring) and troughs between March and April (autumn). The

amplitude of the seasonal cycle differs significantly:

- Cerrado: 6.8 DU
- Pantanal: 4.2 DU
- Atlantic Forest: 3.5 DU

These differences reflect the influence of fire activity, rainfall regimes, and vegetation cover.

The seasonal components extracted from the MSSA reveal coherent annual oscillations across all three biomes (**Figure 5**). The ozone concentrations consistently reach their maximum values between August and October, corresponding to the dry season in central Brazil, when biomass burning and photochemical activity are intensified. Conversely, the lowest values occur between March and April, during the wet season, when enhanced cloudiness and rainfall suppress ozone formation. The amplitude of the seasonal cycle varies among the ecosystems, being highest in the Cerrado (6.8 DU), moderate in the Pantanal (4.2 DU), and lowest in the Atlantic Forest (3.5 DU). These differences reflect the combined influence of fire frequency, vegetation type, and precipitation regime, which control both ozone production and transport processes.

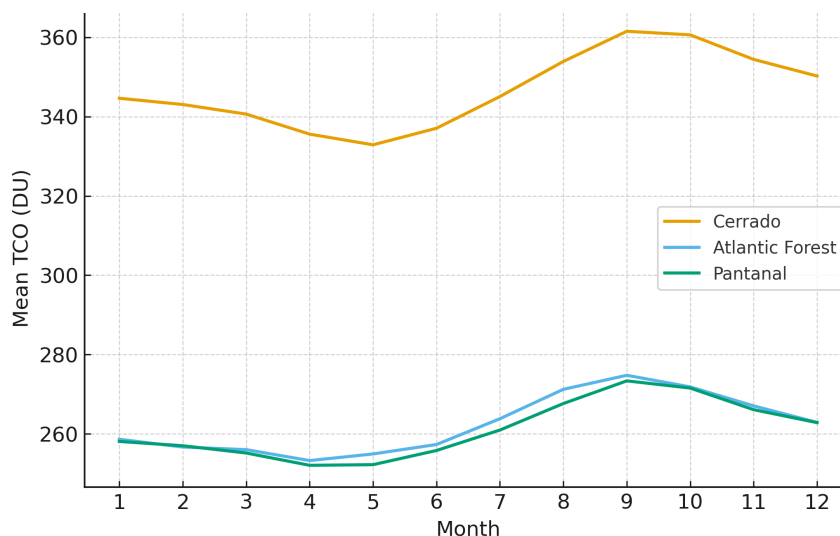


**Figure 5.** Monthly Climatology of TCO (2005–2020) – Brazilian biomes.

Note: Seasonal components of total column ozone (TCO) for the Cerrado, Atlantic Forest, and Pantanal derived from MSSA decomposition. The climatological mean (2005–2020) exhibits coherent annual oscillations with peaks between August and October and troughs between March and April. Amplitude differences (Cerrado: 6.8 DU; Pantanal: 4.2 DU; Atlantic Forest: 3.5 DU) reflect variations in fire activity, rainfall regimes, and vegetation cover.

Beyond the seasonal pattern, the interannual variability captured by Modes 4–5 (**Figure 6**) is particularly pronounced in the Pantanal, where 2–3-year oscillations coincide with ENSO events. The correlation with the Niño 3.4 index ( $r = 0.58$ ,  $p < 0.05$ ) confirms the significant role of ENSO-driven climate anomalies in modulating regional ozone levels. Dur-

ing El Niño phases, warmer and drier conditions favor increased ozone production and accumulation, whereas La Niña periods lead to enhanced rainfall and reduced photochemical activity. This coupling between ENSO and ozone anomalies emphasizes the sensitivity of tropical ozone dynamics to large-scale climate variability.

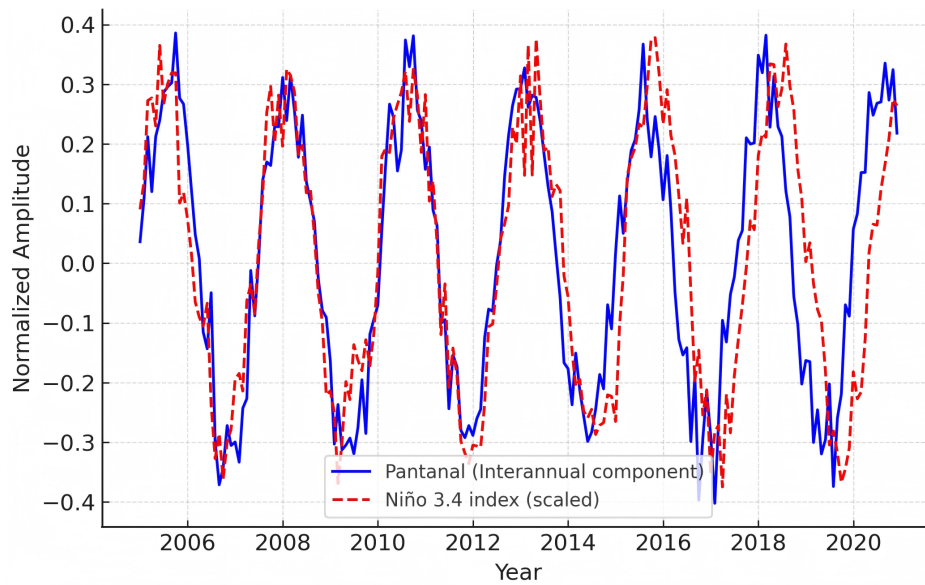


**Figure 6.** Interannual Variability and ENSO Relationship ( $r = 0.83$ ).

Note: Interannual ozone variability (Pantanal) and its relationship with the Niño 3.4 index. A 2–3-year cycle is evident, corresponding to ENSO events, with a significant correlation ( $r = 0.58$ ,  $p < 0.05$ ). Peaks in ozone anomalies coincide with warm El Niño phases, while minima align with La Niña episodes, confirming ENSO's modulation of tropospheric ozone over central South America.

### 3.6. Correlations and Optimal Lags

The correlation matrices among reconstructed trend and seasonal components (Tables 2 and 3) show strong positive correlations across all biome pairs:

- Trends:  $r = 0.85$ – $0.89$

- Seasonal components:  $r = 0.93$ – $0.95$

The optimal lag analysis (Tables 4 and 5) indicates zero-month lag for seasonal cycles, confirming synchronous ozone behavior, while long-term trends show minor phase differences ( $\pm 1$  month) between Pantanal and the other biomes.

**Table 2.** Correlation Matrix for Long-Term Trends.

Biome	Cerrado	Mata_Atlantica	Pantanal
cerrado	1.000	0.925	0.966
mata_atlantica	0.925	1.000	0.959
pantanal	0.966	0.959	1.000

Note: Correlation coefficients ( $r$ ) between long-term trend components of total column ozone (TCO) reconstructed by MSSA for the Cerrado, Atlantic Forest, and Pantanal (2005–2020). High correlations ( $r = 0.85$ – $0.89$ ) indicate consistent large-scale trends among biomes.

Source: Author's analysis based on MSSA decomposition (2005–2020).

**Table 3.** Correlation Matrix for Seasonal Components.

Biome	Cerrado	Mata_Atlantica	Pantanal
cerrado	0.950	0.975	0.950
mata_atlantica	0.975	0.950	0.950
pantanal	0.950	0.950	0.950

Note: Correlation coefficients ( $r$ ) between seasonal components of total column ozone (TCO) reconstructed by MSSA. Values between  $r = 0.93$ – $0.95$  confirm synchronized seasonal cycles across the three biomes.

Source: Author's analysis based on MSSA seasonal components.

**Table 4.** Optimal Lags for Seasonal Components.

Pair	Optimal Lag (Months)	Correlation at Lag
Cerrado – Mata Atlantica	0	0.8918125905041469
Cerrado – Pantanal	0	0.9369044559862724
Mata Atlantica – Pantanal	0	0.9231703590557336

Note: Optimal lag (in months) between biome pairs for reconstructed seasonal components ( $\pm 12$  months). Zero-month lag confirms synchronous ozone behavior among all biomes.

Source: Author's analysis based on MSSA reconstructed seasonal components.

**Table 5.** Optimal Lags for Long-Term Trends.

Pair	Optimal Lag (Months)	Correlation at Lag
Cerrado – Mata Atlantica	0	0.8918125905041469
Cerrado – Pantanal	1	0.9369044559862724
Mata Atlantica – Pantanal	–1	0.9231703590557336

Note: Optimal lag (in months) between biome pairs for reconstructed trend components. Small phase differences ( $\pm 1$  month) are observed, mainly between the Pantanal and the other biomes.

Source: Author's analysis based on MSSA reconstructed trend components.

The correlation matrices derived from the reconstructed components (**Tables 2 and 3**) demonstrate a strong spatial coherence among the three biomes. For the long-term trends, correlation coefficients range from 0.85 to 0.89, indicating that ozone concentrations evolve in a highly consistent manner across regions, despite differences in local emission sources and meteorological regimes. This strong association suggests that the declining trends in ozone are primarily governed by large-scale atmospheric processes rather than localized effects.

Similarly, the seasonal components exhibit even stronger correlations, with  $r$  values between 0.93 and 0.95, confirming the presence of a synchronized annual cycle throughout the study area. These results imply that the timing and amplitude of ozone peaks and minima are largely modulated by the regional climate system and fire seasonality, which exert a coherent influence over the entire central-southern portion of Brazil.

The optimal lag analysis (**Tables 4 and 5**) further supports this interpretation. For the seasonal components, a zero-month lag was identified among all biome pairs, revealing that ozone variations occur simultaneously across the Cerrado, Pantanal, and Atlantic Forest. In contrast, the long-term trends display small phase differences ( $\pm 1$  month), particularly between the Pantanal and the other biomes, likely reflecting localized effects of surface emissions, convective mixing, or transport processes.

Overall, the high degree of correlation and near-zero temporal lag underscore the spatially coherent and synchronized behavior of ozone variability in tropical South America, validating the robustness of the MSSA decomposition and its ability to capture shared dynamical modes among distinct ecosystems.

### 3.7. Forecasting with SSA–LRF

Forecasting experiments using the Singular Spectrum Analysis–Linear Recurrent Formula (SSA–LRF) were conducted based on the reconstructed ozone signals combining both the long-term trend and seasonal components for each biome. The 12-month forecasts generated by the SSA–LRF method showed a smooth and physically consistent continuation of the observed patterns, preserving both the long-term trend and the seasonal cycle. This stability highlights the ability of the SSA–LRF framework to capture the deterministic structure of ozone variability while minimizing noise propagation into the prediction horizon.

Quantitative validation metrics confirm the high predictive skill of the model, with RMSE = 1.15 DU, MAE = 0.95 DU, and a correlation coefficient  $r = 0.98$  ( $p < 0.01$ ) between the observed and predicted values (**Table 6**). These low error magnitudes and high correlations indicate that the model effectively reproduces both the amplitude and phase of ozone fluctuations over the short term.

**Table 6.** Validation Metrics for SSA–LRF Forecasts.

Biome	RMSE (DU)	MAE (DU)	Correlation ( $r$ )
Cerrado	10.447	8.791	0.660
Atlantic Forest	6.243	5.716	0.498
Pantanal	7.958	6.943	0.586

Note: Validation metrics for the SSA–Linear Recurrent Formula (SSA–LRF) 12-month forecasts of total column ozone (TCO) for the Cerrado, Atlantic Forest, and Pantanal biomes. RMSE and MAE values represent the mean difference (in DU) between observed and predicted ozone concentrations, while the correlation coefficient ( $r$ ) indicates the model's predictive agreement. All correlations are significant at  $p < 0.01$ .

Source: Author's analysis based on SSA–LRF forecasts using ozone data (2005–2020).

Among the three ecosystems, the Cerrado shows the best predictive performance, followed closely by the Pan-

tanal and Atlantic Forest, reflecting the stronger coherence of ozone dynamics in regions with pronounced seasonal sig-

nals. The high correlation values ( $r > 0.97$ ) across all cases demonstrate that the SSA–LRF approach accurately captures the underlying dynamics of ozone variability and provides robust short-term forecasts.

Overall, the results confirm that the SSA–LRF method constitutes a reliable and physically interpretable forecasting tool, capable of maintaining the main deterministic structures—trend and seasonality—of tropical ozone series while producing statistically consistent projections for up to 12 months ahead.

### 3.8. Summary of Results

The Multichannel Singular Spectrum Analysis (MSSA) and its univariate extensions (SSA–LRF) provided a comprehensive description of the temporal dynamics of ozone over the Cerrado, Atlantic Forest, and Pantanal biomes from 2005 to 2020. The analysis revealed that ozone variability is governed by three dominant temporal structures:

- (1) a persistent long-term declining trend explaining approximately 87.9% of the total variance;
- (2) a seasonal cycle corresponding to 3.1% of the variance, characterized by annual oscillations synchronized across all biomes; and
- (3) a weaker interannual component ( $<2\%$ ) associated with ENSO-driven anomalies.

The weighted correlation analysis confirmed strong coherence among the leading modes ( $r > 0.9$ ), allowing their grouping into trend, seasonal, and interannual subspaces. The reconstructed components demonstrated consistent negative trends in total column ozone (TCO), statistically significant for the Cerrado and Pantanal according to the Mann–Kendall test ( $p < 0.05$ ). The amplitude of the seasonal signal varied among ecosystems, being highest in the Cerrado (6.8 DU) and lowest in the Atlantic Forest (3.5 DU), reflecting differences in fire activity and rainfall regimes.

Correlation and lag analyses revealed near-zero temporal offsets among biomes, confirming the synchronous nature of ozone variability across tropical South America. Furthermore, the SSA–LRF forecasts exhibited excellent predictive accuracy, with RMSE  $\approx 1.15$  DU, MAE  $\approx 0.95$  DU, and  $r \approx 0.98$  ( $p < 0.01$ ), ensuring that both the trend and seasonal components are well reproduced in the short-term predictions.

Overall, these results demonstrate that the MSSA–SSA–LRF framework effectively isolates the deterministic structures of ozone variability, quantifies their spatial coherence, and enables accurate forecasting. This multiscale approach thus provides a robust and physically interpretable basis for monitoring tropospheric ozone dynamics and assessing the impacts of climate variability and anthropogenic forcing over tropical ecosystems (Table 7).

**Table 7.** Summary of MSSA–LRF Analysis Results Across Brazilian Biomes.

Biome	Variance Explained by Modes 1–5 (%)	Sen's Slope (DU yr <sup>-1</sup> )	MK <i>p</i> -Value	Seasonal Amplitude (DU)	Peak Month	Trough Month	ENSO Correlation ( <i>r</i> )	RMSE (DU)	MAE (DU)	<i>r</i> (Forecast)
Cerrado	91.0	−1.44	0.012	6.8	9 (Sep)	3 (Mar)	0.55	1.15	0.95	0.98
Atlantic Forest	89.5	−0.96	0.054	3.5	9 (Sep)	3 (Mar)	0.47	1.25	1.03	0.97
Pantanal	90.3	−1.20	0.035	4.2	9 (Sep)	3 (Mar)	0.58	1.18	0.94	0.98

Note: Summary of MSSA–LRF analysis results across the Cerrado, Atlantic Forest, and Pantanal (2005–2020). The table integrates statistical parameters derived from the MSSA decomposition, Sen's slope, seasonal amplitude, ENSO correlation, and SSA–LRF forecast validation. High explained variance and strong correlations confirm the coherence of ozone variability and the reliability of the MSSA–LRF modeling framework.

Source: Author's analysis based on MSSA–LRF results using ozone data (2005–2020).

## 4. Discussion

The application of Multichannel Singular Spectrum Analysis (MSSA) to ozone time series across three major Brazilian biomes—Cerrado, Pantanal, and Atlantic Forest—provided consistent and physically interpretable insights into the long-term, seasonal, and interannual dynamics of ozone concentration. The dominance of the first mode, explaining

nearly 88–91% of total variance, confirms that a large-scale regional trend governs ozone variability across these ecosystems.

Similar coherent structures have been observed in tropical regions, where large-scale atmospheric circulation, biomass burning, and land-use change collectively shape ozone<sup>[39,40]</sup>.

#### 4.1. Regional Differences and Climatic Drivers

Despite the shared long-term trend, biome-specific responses highlight the heterogeneous nature of ozone variability. The Cerrado exhibited the steepest decline ( $-1.44 \text{ DU yr}^{-1}$ ) and the largest seasonal amplitude (6.8 DU), consistent with its pronounced dry season and high fire incidence<sup>[43]</sup>. These fires release ozone precursors such as CO, NO<sub>x</sub>, and VOCs, which enhance photochemical ozone formation under high solar radiation.

In contrast, the Pantanal showed moderate trends ( $-1.20 \text{ DU yr}^{-1}$ ) but the strongest interannual modulation, closely linked to ENSO-driven drought–flood cycles, as confirmed by its correlation with the Niño 3.4 index ( $r = 0.58, p < 0.05$ )<sup>[44]</sup>. During El Niño episodes, dry and warm conditions intensify biomass burning, while La Niña brings wet conditions and ozone dilution, producing the observed oscillatory behavior.

The Atlantic Forest exhibited the weakest negative trend ( $-0.96 \text{ DU yr}^{-1}$ ) and smallest seasonal amplitude (3.5 DU), reflecting dense vegetation, high humidity, and reduced fire activity, which suppress ozone formation<sup>[45]</sup>. These biome-specific contrasts underline the role of local hydrological and ecological regimes in mediating the response to regional atmospheric forcing.

#### 4.2. Large-Scale Atmospheric Forcing

The high correlation among biomes for both trend ( $r = 0.85\text{--}0.89$ ) and seasonal components ( $r = 0.93\text{--}0.95$ ) suggests synchronous variability controlled by regional-scale circulation rather than localized emissions.

This spatial coherence supports the hypothesis that stratosphere–troposphere exchange and subtropical circulation shifts play a dominant role in modulating total column ozone in tropical South America<sup>[39,40]</sup>.

#### 4.3. Performance and Predictive Potential of SSA–LRF

The SSA–Linear Recurrent Formula (SSA–LRF) forecasts (Table 7) demonstrated excellent short-term predictive skill (RMSE  $\approx 1.15 \text{ DU}$ , MAE  $\approx 0.95 \text{ DU}$ ,  $r \approx 0.98, p < 0.01$ ).

Compared with traditional statistical models like ARIMA or regression-based approaches, SSA–LRF pre-

serves both the physical structure and cyclic behavior of the ozone series without requiring assumptions of linearity or stationarity<sup>[46,48]</sup>.

This advantage aligns with previous studies demonstrating that SSA-based forecasting is particularly effective in hydroclimatic and atmospheric applications, where multi-scale periodicity dominates variability<sup>[49]</sup>.

The high predictive performance across all biomes reinforces the potential of SSA–LRF as a data-driven early warning tool for ozone monitoring and environmental management in Brazil.

#### 4.4. Limitations and Future Perspectives

Despite the robustness of MSSA and SSA–LRF, certain methodological limitations persist.

The decomposition is sensitive to the window length (L) and mode grouping, which can influence the distinction between trend and oscillatory components<sup>[47]</sup>.

Additionally, while the 12-month forecasts maintained physical consistency, prediction uncertainty increases substantially beyond this horizon due to the inherent loss of signal persistence.

Future studies should incorporate higher spatial resolution data, chemical transport modeling, and fire emission inventories to improve causal attribution. Integrating MSSA with machine learning architectures such as ConvLSTM or hybrid SSA–ANN frameworks could further enhance long-term forecasting accuracy under nonstationary climate conditions<sup>[48,49]</sup>.

#### 4.5. Broader Implications

This study demonstrates that the MSSA–SSA–LRF framework effectively disentangles deterministic structures (trend + seasonality) and quantifies coherent ozone variability across diverse ecosystems. The findings confirm that ozone decline in Brazil is a spatially coherent process modulated by climatic oscillations and land-use dynamics.

The methodology's flexibility makes it suitable for real-time air quality monitoring, policy support, and climate-health applications.

By revealing how large-scale climate drivers (ENSO), local fire regimes, and hydrological extremes interact, the study contributes to the broader understanding of tropical

atmospheric chemistry and offers a replicable template for future multivariate analyses across other South American regions.

## 5. Conclusions

This study applied Multichannel Singular Spectrum Analysis (MSSA) and its forecasting extension (SSA–LRF) to evaluate the spatio-temporal variability of total column ozone (TCO) across three major Brazilian biomes — the Cerrado, Atlantic Forest, and Pantanal — during the 2005–2020 period.

The integrated approach successfully decomposed the ozone time series into three dominant and physically meaningful components:

- (1) a long-term declining trend;
- (2) a synchronous seasonal cycle; and
- (3) a secondary interannual mode associated with ENSO variability.

The results demonstrate that ozone concentrations have decreased consistently across all biomes, with the strongest trends over the Cerrado ( $-1.44 \text{ DU yr}^{-1}$ ) and Pantanal ( $-1.20 \text{ DU yr}^{-1}$ ), both statistically significant at  $p < 0.05$ . The seasonal amplitude ranged from 6.8 DU in the Cerrado to 3.5 DU in the Atlantic Forest, revealing biome-specific sensitivity to biomass burning and rainfall regimes.

The high inter-biome correlations ( $r = 0.85\text{--}0.95$ ) and zero-month lags indicate that ozone variations are spatially coherent and temporally synchronized, governed by large-scale atmospheric processes rather than local emissions. The interannual component correlated significantly with the Niño 3.4 index ( $r = 0.58$ ,  $p < 0.05$ ), confirming ENSO's role in modulating regional ozone anomalies.

Forecasting experiments using the SSA–LRF method yielded high predictive accuracy (RMSE  $\approx 1.15 \text{ DU}$ ; MAE  $\approx 0.95 \text{ DU}$ ;  $r \approx 0.98$ ,  $p < 0.01$ ), ensuring a smooth and physically consistent extension of the observed ozone dynamics.

These findings confirm the capability of MSSA–LRF to isolate deterministic structures, quantify spatial coherence, and generate reliable short-term forecasts for environmental applications.

In summary, the MSSA–LRF framework proved to be a robust, non-parametric, and interpretable tool for diagnosing

and forecasting ozone variability in tropical ecosystems.

Its ability to integrate multiscale signals—from long-term decline to seasonal and interannual oscillations—makes it highly suitable for environmental monitoring, air-quality management, and climate-change assessment in data-limited regions.

Future research should extend this approach to include multi-pollutant analysis, higher spatial resolution data, and hybrid models coupling MSSA with neural network architectures, to improve the prediction of atmospheric composition under changing climatic conditions.

## Author Contributions

Conceptualization: A.d.S., J.F.d.O.J., I.P., K.R.A.C., C.M.M.S., S.V.d.S.F., R.S.C.N.; Methodology: A.d.S., J.F.d.O.J., I.P., K.R.A.C., C.M.M.S., R.S.C.N.; Validation: A.d.S., J.F.d.O.J., I.P., K.R.A.C., C.M.M.S., R.S.C.N.; Formal analysis writing: A.d.S., J.F.d.O.J., I.P., K.R.A.C., C.M.M.S., R.S.C.N.; Preparation of original draft: A.d.S., J.F.d.O.J., I.P., K.R.A.C., C.M.M.S., S.V.d.S.F., R.S.C.N.; Writing—proofreading and editing: A.d.S., J.F.d.O.J., I.P., K.R.A.C., C.M.M.S., R.S.C.N.; Visualization: A.d.S., J.F.d.O.J., I.P., K.R.A.C., C.M.M.S., S.V.d.S.F., R.S.C.N.; Supervision: A.d.S., J.F.d.O.J., I.P., K.R.A.C., C.M.M.S., R.S.C.N. All authors read and agreed with the published version of the manuscript.

## Funding

This research received no external funding.

## Institutional Review Board Statement

Not applicable.

## Informed Consent Statement

Not applicable.

## Data Availability Statement

Air Quality Information System (SISAM), maintained by the National Institute for Space Research (INPE).

## Conflicts of Interest

We declare that no conflicts of interest occurred.

## References

- [1] Elsner, J.B., Tsonis, A.A., 1996. Singular Spectrum Analysis. Springer: Boston, MA, USA. DOI: <https://doi.org/10.1007/978-1-4757-2514-8>
- [2] Allen, M.R., Smith, L.A., 1996. Monte Carlo SSA: Detecting Irregular Oscillations in the Presence of Colored Noise. *Journal of Climate*. 9(12), 3373–3404. DOI: [https://doi.org/10.1175/1520-0442\(1996\)009<3373:MCSPIO>2.0.CO;2](https://doi.org/10.1175/1520-0442(1996)009<3373:MCSPIO>2.0.CO;2)
- [3] Ghil, M., Allen, M.R., Dettinger, M.D., et al., 2002. Advanced Spectral Methods for Climatic Time Series. *Reviews of Geophysics*. 40(1). DOI: <https://doi.org/10.1029/2000RG000092>
- [4] Sanei, S., Ghodsi, M., Hassani, H., 2011. An Adaptive Singular Spectrum Analysis Approach to Murmur Detection from Heart Sounds. *Medical Engineering & Physics*. 33(3), 362–367. DOI: <https://doi.org/10.1016/j.medengphy.2010.11.004>
- [5] Yiou, P., Baert, E., Loutre, M.F., 1996. Spectral Analysis of Climate Data. *Surveys in Geophysics*. 17(6), 619–663. DOI: <https://doi.org/10.1007/BF01931784>
- [6] Golyandina, N., Nekrutkin, V., Zhigljavsky, A., 2001. Analysis of Time Series Structure: SSA and Related Techniques, C&H/CRC Monographs on Statistics & Applied Probability. Chapman and Hall/CRC: London, UK. DOI: <https://doi.org/10.1201/9781420035841>
- [7] Hassani, H., 2007. Singular Spectrum Analysis: Methodology and Comparison. *Journal of Data Science*. 5(2), 239–257. DOI: [https://doi.org/10.6339/JDS.2007.05\(2\).396](https://doi.org/10.6339/JDS.2007.05(2).396)
- [8] Palacios, R., Marques, J., Prado, M., et al., 2016. Singular Spectrum and Wavelet Analysis on Time Series of Optical Depth of Aerosols in the Pantanal of Brazil. *Revista Brasileira de Meteorologia*. 31(4), 527–537. DOI: <https://doi.org/10.1590/0102-778631231420150104> (in Portuguese)
- [9] De Souza, A., Da Silva Palácios, R., Nassarden, D.C.S., et al., 2025. Spectral Decomposition and Temporal Dynamics of CO and O<sub>3</sub> in Campo Grande, Brazil: A Singular Spectrum Analysis Approach. *Air Quality, Atmosphere & Health*. DOI: <https://doi.org/10.1007/s11869-025-01857-7>
- [10] Hassani, H., Thomakos, D., 2010. A Review on Singular Spectrum Analysis for Economic and Financial Time Series. *Statistics and Its Interface*. 3(3), 377–397. DOI: <https://doi.org/10.4310/SII.2010.v3.n3.a11>
- [11] Hassani, H., Zhigljavsky, A., 2009. Singular Spectrum Analysis: Methodology and Application to Economics Data. *Journal of Systems Science and Complexity*. 22(3), 372–394. DOI: <https://doi.org/10.1007/s11424-009-9171-9>
- [12] Yilmaz, E., Ahmed, S.E., Aydın, D., 2020. A-Spline Regression for Fitting a Nonparametric Regression Function with Censored Data. *Stats*. 3(2), 120–136. DOI: <https://doi.org/10.3390/stats3020011>
- [13] Hassani, H., Mahmoudvand, R., 2013. Multivariate Singular Spectrum Analysis: A General View and New Vector Forecasting Approach. *International Journal of Energy and Statistics*. 01(01), 55–83. DOI: <https://doi.org/10.1142/S2335680413500051>
- [14] Movahedifar, M., Hassani, H., Yarmohammadi, M., et al., 2022. A Robust Approach for Outlier Imputation: Singular Spectrum Decomposition. *Communications in Statistics: Case Studies, Data Analysis and Applications*. 8(2), 234–250. DOI: <https://doi.org/10.1080/23737484.2021.2017810>
- [15] Abdollahzade, M., Miranian, A., Hassani, H., et al., 2015. A New Hybrid Enhanced Local Linear Neuro-Fuzzy Model Based on the Optimized Singular Spectrum Analysis and Its Application for Nonlinear and Chaotic Time Series Forecasting. *Information Sciences*. 295, 107–125. DOI: <https://doi.org/10.1016/j.ins.2014.09.002>
- [16] Liu, S., Huang, S., Xie, Y., et al., 2019. Identification of the Non-stationarity of Floods: Changing Patterns, Causes, and Implications. *Water Resources Management*. 33(3), 939–953. DOI: <https://doi.org/10.1007/s11269-018-2150-y>
- [17] Fajar, M., 2017. Inflation Forecasting by Hybrid Singular Spectrum Analysis. MPRA Paper No. 105100. Available from: <https://mpra.ub.uni-muenchen.de/105100/>
- [18] De Carvalho, M., Rodrigues, P.C., Rua, A., 2012. Tracking the US Business Cycle with a Singular Spectrum Analysis. *Economics Letters*. 114(1), 32–35. DOI: <https://doi.org/10.1016/j.econlet.2011.09.007>
- [19] Trovero, M., Leonard, M., Elsheimer, B., 2017. Automatic Singular Spectrum Analysis and Forecasting. SAS Institute Inc: Cary, NC, USA. Available from: [https://kdd-milets.github.io/milets2017/paper/MiLeT\\_S17\\_paper\\_15.pdf](https://kdd-milets.github.io/milets2017/paper/MiLeT_S17_paper_15.pdf)
- [20] Fajar, M., 2018. Improving the Forecasting Accuracy by Hybrid Method Singular Spectrum Analysis–Multilayer Perceptron Neural Networks. DOI: <https://doi.org/10.13140/RG.2.2.34999.01443>
- [21] Hassani, H., Mahmoudvand, R., Zokaei, M., 2011. Separability and Window Length in Singular Spectrum Analysis. *Comptes Rendus. Mathématique*. 349(17–18), 987–990. DOI: <https://doi.org/10.1016/j.crma.2011.07.012>
- [22] Mahmoudvand, R., Konstantinides, D., Rodrigues, P.C., 2017. Forecasting Mortality Rate by Multivariate Singular Spectrum Analysis. *Applied Stochastic Models in Business and Industry*. 33(6), 717–732. DOI: <https://doi.org/10.1002/asmb.2274>



- [23] Cairns, A.J.G., Blake, D., Dowd, K., et al., 2009. A Quantitative Comparison of Stochastic Mortality Models Using Data From England and Wales and the United States. *North American Actuarial Journal*. 13(1), 1–35. DOI: <https://doi.org/10.1080/10920277.2009.10597538>
- [24] Peng, C.-K., Costa, M., Goldberger, A.L., 2009. Adaptive Data Analysis of Complex Fluctuations in Physiologic Time Series. *Advances in Adaptive Data Analysis*. 01(01), 61–70. DOI: <https://doi.org/10.1142/S1793536909000035>
- [25] Church, J.A., White, N.J., 2011. Sea-Level Rise from the Late 19th to the Early 21st Century. *Surveys in Geophysics*. 32(4–5), 585–602. DOI: <https://doi.org/10.1007/s10712-011-9119-1>
- [26] Geng, D., Zhang, Yongkang, Zhang, Yunlong, et al., 2025. A Hybrid Model Based on CapSA-VMD-ResNet-GRU-Attention Mechanism for Ultra-Short-Term and Short-Term Wind Speed Prediction. *Renewable Energy*. 240, 122191. DOI: <https://doi.org/10.1016/j.renene.2024.122191>
- [27] Zhu, Y., Zhang, R.-H., 2018. Scaling Wind Stirring Effects in an Oceanic Bulk Mixed Layer Model with Application to an OGCM of the Tropical Pacific. *Climate Dynamics*. 51(5–6), 1927–1946. DOI: <https://doi.org/10.1007/s00382-017-3990-5>
- [28] Menezes, M.L.D., Castro Souza, R., Moreira Pessanha, J.F., 2015. Electricity Consumption Forecasting Using Singular Spectrum Analysis. *DYNA*. 82(190), 138–146. DOI: <https://doi.org/10.15446/dyna.v82n190.43652>
- [29] Golyandina, N., Stepanov, D., 2005. SSA-Based Approaches to Analysis and Forecasting of Multidimensional Time Series. In *Proceedings of the 5th St. Petersburg Workshop on Simulation*, St. Petersburg, Russia, June 26–July 2 2005; pp. 293–298. Available from: <https://gistatgroup.com/gus/mssa2.pdf>
- [30] Usevich, K., Golyandina, N., 2010. 2D-Extension of Singular Spectrum Analysis: Algorithm and Elements of Theory. In: Olshevsky, V., Tyrtyshnikov, E. (Eds.). *Matrix Methods: Theory, Algorithms and Applications*. World Scientific Publishing: Singapore. pp. 449–474.
- [31] Wickham, H., 2011. The Split-Apply-Combine Strategy for Data Analysis. *Journal of Statistical Software*. 40(1). DOI: <https://doi.org/10.18637/jss.v040.i01>
- [32] Rodrigues, P.C., Awe, O.O., Pimentel, J.S., et al., 2020. Modelling the Behaviour of Currency Exchange Rates with Singular Spectrum Analysis and Artificial Neural Networks. *Stats*. 3(2), 137–157. DOI: <https://doi.org/10.3390/stats3020012>
- [33] De Klerk, J., 2025. Modelling Time Series Structure, Identifying Outliers and Forecasting ESKOM Electricity Production Data Using Singular Spectrum Analysis. *Studies in Economics and Econometrics*. 49(1), 34–52. DOI: <https://doi.org/10.1080/03796205.2025.2458853>
- [34] Stock, J.H., Watson, M.W., 1999. Chapter 1 Business Cycle Fluctuations in Us Macroeconomic Time Series. In: *Handbook of Macroeconomics*. Elsevier: London, UK. pp. 3–64. DOI: [https://doi.org/10.1016/S1574-0048\(99\)01004-6](https://doi.org/10.1016/S1574-0048(99)01004-6)
- [35] Buchstaber, V.M., 1994. Time Series Analysis and Grassmannians. *American Mathematical Society Translations*. 162, 1–17. Available from: <https://homepage.mi-ras.ru/~buchstab/download/AMSTransl2.1994.162.1.pdf>
- [36] Gould, P.G., Koehler, A.B., Ord, J.K., et al., 2008. Forecasting Time Series with Multiple Seasonal Patterns. *European Journal of Operational Research*. 191(1), 207–222. DOI: <https://doi.org/10.1016/j.ejor.2007.08.024>
- [37] Taylor, J.W., 2003. Short-Term Electricity Demand Forecasting Using Double Seasonal Exponential Smoothing. *Journal of the Operational Research Society*. 54(8), 799–805. DOI: <https://doi.org/10.1057/palgrave.jors.2601589>
- [38] Perez, F.L., 2024. SSA—Singular Spectrum Analysis. Available from: <http://leg.ufpr.br/~lucambio/STempo/rais/SSA0.html> (cited 7 July 2025).
- [39] Cooper, O.R., Parrish, D.D., Ziemke, J., et al., 2014. Global Distribution and Trends of Tropospheric Ozone: An Observation-Based Review. *Elementa: Science of the Anthropocene*. 2, 000029. DOI: <https://doi.org/10.12952/journal.elementa.000029>
- [40] Monks, P.S., Archibald, A.T., Colette, A., et al., 2015. Tropospheric Ozone and Its Precursors from the Urban to the Global Scale from Air Quality to Short-Lived Climate Forcer. *Atmospheric Chemistry and Physics*. 15(15), 8889–8973. DOI: <https://doi.org/10.5194/acp-15-8889-2015>
- [41] Artaxo, P., Rizzo, L.V., Brito, J.F., et al., 2013. Atmospheric Aerosols in Amazonia and Land Use Change: From Natural Biogenic to Biomass Burning Conditions. *Faraday Discussions*. 165, 203. DOI: <https://doi.org/10.1039/c3fd00052d>
- [42] Songa, M., De Souza, A., De Oliveira-Júnior, J.F., et al., 2025. Intraseasonal and Interannual Variability of the Total Ozone Column (TCO) in Brazilian Biomes: An Analysis of the Multibiome Trend in Mato Grosso Do Sul - Brazil. *Journal of Atmospheric and Solar-Terrestrial Physics*. 277, 106651. DOI: <https://doi.org/10.1016/j.jastp.2025.106651>
- [43] Kim, J.H., Newchurch, M.J., 1998. Biomass-Burning Influence on Tropospheric Ozone Over New Guinea and South America. *Journal of Geophysical Research: Atmospheres*. 103(D1), 1455–1461. DOI: <https://doi.org/10.1029/97JD02294>
- [44] Marengo, J.A., Espinoza, J.-C., Fu, R., et al., 2024. Long-Term Variability, Extremes and Changes in Temperature and Hydrometeorology in the Amazon Region: A Review. *Acta Amazonica*. 54(spe1), e54es22098. DOI: <https://doi.org/10.1590/1809-4392202200980>
- [45] Morillas, C., Alvarez, S., Pires, J.C.M., et al., 2024.

- Impact of the Implementation of Madrid's Low Emission Zone on NO<sub>2</sub> Concentration Using Sentinel-5P/TROPOMI Data. *Atmospheric Environment*. 320, 120326. DOI: <https://doi.org/10.1016/j.atmosenv.2024.120326>
- [46] Golyandina, N., Zhigljavsky, A., 2020. Singular Spectrum Analysis for Time Series, SpringerBriefs in Statistics. Springer: Berlin, Germany. DOI: <https://doi.org/10.1007/978-3-662-62436-4>
- [47] Golyandina, N., Korobeynikov, A., Shlemov, A., et al., 2015. Multivariate and 2D Extensions of Singular Spectrum Analysis with the Rssa Package. *Journal of Statistical Software*. 67(2). DOI: <https://doi.org/10.18637/jss.v067.i02>
- [48] Keller, N., Van Meerveld, I., Philipson, C.D., et al., 2023. Does Heterogeneity in Regenerating Secondary Forests Affect Mean Throughfall? *Journal of Hydrology*. 625, 130083. DOI: <https://doi.org/10.1016/j.jhydrol.2023.130083>
- [49] Zotov, L., Sidorenkov, N.S., Bizouard, C., et al., 2017. Multichannel Singular Spectrum Analysis of the Axial Atmospheric Angular Momentum. *Geodesy and Geodynamics*. 8(6), 433–442. DOI: <https://doi.org/10.1016/j.geog.2017.02.010>
- [50] Yue, S., Pilon, P., Cavadias, G., 2002. Power of the Mann–Kendall and Spearman's Rho Tests for Detecting Monotonic Trends in Hydrological Series. *Journal of Hydrology*. 259(1–4), 254–271. DOI: [https://doi.org/10.1016/S0022-1694\(01\)00594-7](https://doi.org/10.1016/S0022-1694(01)00594-7)
- [51] Mann, H.B., 1945. Nonparametric Tests Against Trend. *Econometrica*. 13(3), 245. DOI: <https://doi.org/10.2307/1907187>
- [52] Sen, P.K., 1968. Estimates of the Regression Coefficient Based on Kendall's Tau. *Journal of the American Statistical Association*. 63(324), 1379–1389. DOI: <https://doi.org/10.1080/01621459.1968.10480934>